

Meta-Reinforcement Learning With Mixture of Experts for Generalizable Multi Access in Heterogeneous Wireless Networks

Zhaoyang Liu, Xijun Wang, Chenyuan Feng, Xinghua Sun, Wen Zhan, and Xiang Chen

Abstract—This paper focuses on spectrum sharing in heterogeneous wireless networks, where nodes with different Media Access Control (MAC) protocols to transmit data packets to a common access point over a shared wireless channel. While previous studies have proposed Deep Reinforcement Learning (DRL)-based multiple access protocols tailored to specific scenarios, these approaches are limited by their inability to generalize across diverse environments, often requiring time-consuming retraining. To address this issue, we introduce Generalizable Multiple Access (GMA), a novel Meta-Reinforcement Learning (meta-RL)-based MAC protocol designed for rapid adaptation across heterogeneous network environments. GMA leverages a context-based meta-RL approach with Mixture of Experts (MoE) to improve representation learning, enhancing latent information extraction. By learning a meta-policy during training, GMA enables fast adaptation to different and previously unknown environments, without prior knowledge of the specific MAC protocols in use. Simulation results demonstrate that, although the GMA protocol experiences a slight performance drop compared to baseline methods in training environments, it achieves faster convergence and higher performance in new, unseen environments.

Index Terms—Media Access Control, heterogeneous wireless network, meta reinforcement learning, mixture of expert.

I. INTRODUCTION

In contemporary wireless environments, multiple network types with distinct characteristics, such as 5G, WiFi, and IoT networks, coexist within the same physical space, each using different Media Access Control (MAC) protocols. This diversity presents significant challenges for spectrum sharing and interference management. Traditionally, networks have relied on pre-allocating exclusive frequency bands, a method that often leads to inefficient spectrum utilization. As wireless technologies continue to proliferate, the demand for wireless communication services is outpacing the availability of spectrum resources. To address this, the Defense Advanced Research Projects Agency (DARPA) introduced the Spectrum Collaboration Challenge (SC2) competition [2], [3], proposing a novel spectrum-sharing paradigm. In this approach, co-located, heterogeneous networks collaborate to share spectrum

without requiring prior knowledge of each other's MAC protocols. SC2 encourages the development of intelligent systems capable of adapting in real-time to dynamic and congested spectrum environments. A key solution to this challenge lies in developing intelligent MAC protocols for a particular network among those sharing the spectrum, enabling efficient and equitable spectrum sharing.

Several Deep Reinforcement Learning (DRL) based multiple access schemes have been developed for coexistence with heterogeneous wireless networks [4]–[13]. One notable protocol in this area is the Deep Reinforcement Learning Multiple Access (DLMA) proposed by Yu *et al.* [4], which utilizes Deep Q-Network (DQN) [14] to learn the access policy. Specifically, the DRL agent in DLMA makes access decisions based on historical data to enable coexistence with other nodes that use different MAC protocols. The DRL-based multiple access scheme can effectively learn to coexist with other MAC protocols in specific pre-determined heterogeneous wireless network scenarios. However, a key challenge that remains unaddressed is the ability to generalize DRL performance to unseen testing environments that differ from the training environments. In real-world deployments, the heterogeneous wireless network composition, including the number of nodes and MAC protocols employed, is likely to vary across different environments. This mismatch between training and testing environments can lead to degraded performance of the DRL agent. While it is possible to train a new DRL model from scratch for each unseen testing environment, this approach is highly inefficient and time-consuming due to the significant effort required to collect sufficient training data and the high sample complexity involved in achieving convergence. Therefore, enhancing the generalization capabilities of DRL agents to maintain robust performance across diverse, unseen heterogeneous wireless environments is a crucial challenge.

In this paper, we investigate harmonious spectrum sharing in co-located heterogeneous wireless networks, where a DRL-based agent node and multiple existing nodes with different MAC protocols share the same wireless channel. Our primary objective is to enhance the generalization capabilities of DRL-based multiple access control across diverse coexistence scenarios, enabling rapid adaptation to previously unseen and dynamic wireless environments. In our prior work [1], we focused solely on maximizing the total throughput of the heterogeneous wireless network, without considering fairness between the agent node and the existing nodes. We expand this research by addressing the critical issue of fairness in

Part of this work was presented at the WiOpt 2023 Workshop on Machine Learning in Wireless Communications [1].

Z. Liu, X. Wang, and X. Chen are with the School of Electronics and Information Technology, Sun Yat-sen University, Guangzhou, China (e-mail: liuzhy86@mail2.sysu.edu.cn; wangxijun@mail.sysu.edu.cn; chenxiang@mail.sysu.edu.cn).

C. Feng is with the Department of Communication Systems, EURECOM, Biot, France. (e-mail: Chenyuan.Feng@eurecom.fr).

X. Sun and W. Zhan are with the School of Electronics and Communication Engineering, Shenzhen Campus of Sun Yat-sen University, Shenzhen, China (e-mail: sunxinghua@mail.sysu.edu.cn; zhanwen6@mail.sysu.edu.cn).

the co-existence scenario, fostering diverse and equitable coordination patterns. Additionally, we incorporate a Mixture of Experts (MoE) architecture into meta Reinforcement Learning (meta-RL) approach to improve task representation capabilities. The key contributions of this paper are summarized as follows:

- We consider a range of heterogeneous wireless environments, treating each as a distinct task in the context of meta-RL. In each environment, we model the multiple access problem in a heterogeneous wireless network as a Markov Decision Process (MDP). To balance the dual objectives of maximizing throughput and ensuring fairness, we define a reward function that considers both system throughput and fairness between the agent node and existing nodes. We further structure the problem within a meta-RL framework to ensure the generalizability of the learned policy across varying network conditions and diverse environments.
- We propose a novel MAC protocol for the agent node, called Generalizable Multiple Access (GMA), which leverages context-based off-policy meta-RL with MoE layers to enhance the agent node’s ability to make intelligent access decisions across diverse network environments. The GMA protocol includes an MoE-enhanced encoder to generate more discriminating task embeddings and uses Soft Actor-Critic (SAC) for learning a goal-conditioned policy. Through this approach, GMA learns a meta-policy based on experiences from a variety of training tasks, rather than task-specific policies. This meta-policy allows GMA to quickly adapt to new tasks or environments, significantly improving convergence speed when faced with previously unseen scenarios.
- Simulation results demonstrate that GMA ensures universal access in well-trained environments, delivers high initial performance in new environments, and rapidly adapts to dynamic conditions. We also show that, with our proposed fairness metric, GMA effectively balances high total throughput with fairness. Through extensive experiments, we explore the impact of training task selection on zero-shot and few-shot performance and provide valuable insights into designing effective meta-learning training sets. Moreover, we highlight the performance improvements enabled by the MoE architecture, underscoring the superiority of our approach, and examine how the number of experts influences system performance.

The remainder of this paper is organized as follows. In Section II, we review related work. Section III details the system model and problem formulation. In Section IV, we present the proposed meta-RL-based MAC protocol. The simulation results are discussed in Section V. Finally, Section VI concludes with the main findings.

II. RELATED WORK

A. DRL in Heterogeneous Wireless Networks

The concept of heterogeneous wireless networks, where diverse communication protocols coexist in the same physical space and share the same spectrum, has emerged as a

promising paradigm to achieve higher spectral efficiency. A wide range of MAC protocol designs for heterogeneous wireless networks have drawn inspiration from DLMA [4], with various extensions proposed to address different coexistence scenarios. In [5], DLMA has been extended to address the multi-channel heterogeneous network access problem, where the DRL agent decides both whether to transmit and which channel to access. A variant called CS-DLMA was introduced in [6], incorporating carrier sensing (CS) capability to enable coexistence with carrier-sense multiple access with collision avoidance (CSMA/CA) protocols. The authors in [7] further introduced a MAC protocol enabling DRL nodes to access the channel without detecting the channel idleness, and assessed the coexistence performance with WiFi nodes. A MAC protocol based on DRL was proposed in [8] to coexist with existing nodes in underwater acoustic communication networks, where high delay in transmissions is a concern. On the basis of [8], the work in [9] further addressed the issue of coexistence with asynchronous transmission protocol nodes in underwater acoustic communication networks. Deng *et al.* [10] proposed an R-learning-based random access scheme specifically designed for coexistence in heterogeneous wireless networks with delay-constrained traffic. For scenarios involving multiple agent nodes, distributed DLMA was introduced in [11] to facilitate the coexistence of multiple agents in heterogeneous wireless networks with imperfect channels. In [13], a novel framework leveraging curriculum learning and multitask reinforcement learning was introduced to enhance the performance of access protocols in dynamic heterogeneous environments. Additionally, a QMIX-based multiple access scheme was proposed for multiple nodes in [15], which also demonstrates compatibility with CSMA/CA protocols. However, the majority of these works neglects challenges in unseen and dynamic environments, rendering the trained policies effective only for scenarios similar to those used in training. Only a few studies, such as [5], [13], have considered this issue, but they solely rely on recurrent neural network and require extensive gradient updates for adaptation in dynamic environments.

B. Fairness Coexistence

Ensuring fairness among nodes with different protocols is crucial in coexistence environments. A common approach is to incorporate the fairness metric directly into the objective function and redesign the reward function to account for fairness considerations. In light of this, DLMA [4] modified the standard Q-learning algorithm by incorporating an α -fairness factor into the Q-value estimate to meet the fairness objective. Frommel *et al.* [16] proposed a DRL approach to dynamically adjust the contention window of 802.11ax stations. They adopted the α -fairness index as the metric of the overall system performance, rather than sum throughput, to simultaneously improve raw data rates in WiFi systems and maintain the fairness between legacy stations and 802.11ax stations. The authors in [17] introduced a mean-field based DRL approach for coexistence with WiFi access points, using a Jain’s fairness index-weighted reward to address the fairness

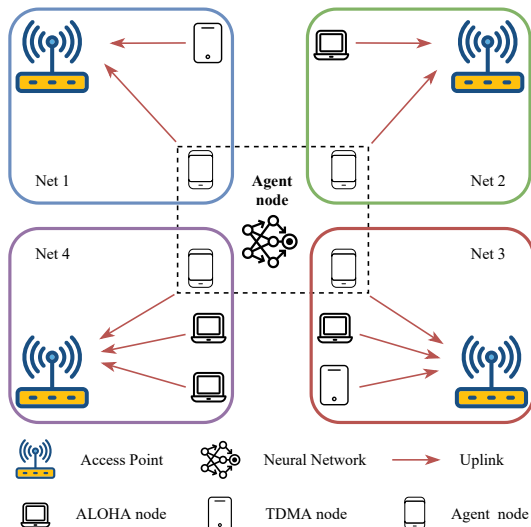


Fig. 1. Heterogeneous wireless networks with diverse coexisting scenarios.

issue in LTE-unlicensed. In [18], the author investigated the fairness of coexistence between unlicensed nodes and Wi-Fi nodes by integrating 3GPP fairness. Tan *et al.* [19] introduced the length of idle ending as an indicator of whether the WiFi system has finished transmitting all buffered packets, incorporating this indicator into the reward function to ensure fair coexistence between license-assisted access LTE systems and WiFi systems. In [15], the authors proposed a delay to last successful transmission (D2LT) indicator and designed the reward function based on D2LT. The reward function encourages the node with the largest delay to transmit, thereby achieving proportional fairness among the nodes. In [13], a reward function was defined to ensure fairness among nodes by assigning additional rewards or penalties based on the sorted index of nodes' throughput, prioritizing those with lower throughput. Additionally, a new metric, the average age of a packet, was proposed in [20] to measure the short-term imbalance among nodes, thereby ensuring short-term fairness. However, most of these studies require prior knowledge of the environments, such as the total number of nodes and the throughput of each node, which limits their applicability in practical scenarios where such information is not available.

III. SYSTEM MODEL AND PROBLEM FORMULATION

In this section, we first present the system model of the heterogeneous wireless network and then formulate the multiple access problem as an MDP.

A. System Model

We investigate a heterogeneous wireless network, where multiple nodes, including N existing nodes and an agent node, transmit packets to an Access Point (AP) through a shared wireless channel. The set of all nodes is denoted by $\{0, 1, \dots, N\}$, where 0 represents the agent node and $\{1, \dots, N\}$ represents the existing nodes. The network is considered heterogeneous because each node may utilize a

different MAC protocol. Importantly, there is no prior knowledge available about the number of existing nodes or the MAC protocols they employ. The system operates in a time-slotted manner, with each time slot corresponding to the duration of a data packet transmission. Nodes are allowed to initiate transmission only at the beginning of a time slot. A packet is considered successfully transmitted if no other nodes transmit simultaneously, and in this case, the AP broadcasts an ACK packet. However, if multiple nodes transmit concurrently in the same time slot, a collision occurs, and the AP broadcasts a NACK packet to indicate an unsuccessful transmission.

In accordance with [4], we consider four types of time-slotted MAC protocols that may be used by existing nodes: q -ALOHA, Fixed-Window ALOHA (FW-ALOHA), Exponential Backoff ALOHA (EB-ALOHA), and Time Division Multiple Access (TDMA). In q -ALOHA, nodes transmit in each time slot with a fixed probability q . In FW-ALOHA, a node generates a random counter in the range of $[0, W - 1]$ after transmitting, and it must wait for the counter to expire before initiating its next transmission. EB-ALOHA is a variant of FW-ALOHA where the window size doubles progressively when collisions occur during transmission. This increase in window size continues until a maximum size $2^b W$ is reached, where b is the maximum backoff stage. After a successful transmission, the window size is reset to its initial value W . TDMA divides time into frames, each consisting of multiple time slots. Nodes are assigned specific time slots within each frame according to a predetermined schedule.

The agent node decides whether to transmit data in each time slot. Upon transmission, it receives immediate feedback from the AP, indicating whether the transmission was successful or not. If the agent node chooses not to transmit, it actively listens to the channel and gathers observations about the environment. These observations provide information about the transmission outcomes of other nodes or the idleness of the channel. The agent node's objective is to maximize overall wireless spectrum utilization across the entire network while ensuring harmonious coexistence with existing nodes. This involves efficiently and fairly utilizing the underutilized channels of existing nodes.

Considering the varying number of existing nodes and the potential use of different MAC protocols, there is a wide range of coexisting scenarios in heterogeneous wireless networks, as depicted in Fig. 1. We aim to design a generalizable MAC protocol that enables the coexistence of the agent node with existing nodes across diverse heterogeneous wireless networks. The protocol offers universal accessibility and rapid adaptation capabilities, allowing the agent node to adjust to different network conditions encountered in heterogeneous environments.

B. MDP formulation

We formulate the multiple access problem for the agent node in heterogeneous wireless networks as an MDP. The components of the MDP are defined as follows.

1) *Action*: The action of the agent node at the beginning of time slot t is denoted by $a_{t,0} \in \{0, 1\}$. For simplicity, we

TABLE I
POSSIBLE ACTION-OBSERVATIONS PAIRS IN EACH TIME SLOT.

a_t	o_t	Description
0	0	The channel is idle.
0	1	An existing node transmits successfully.
0	2	A collision occurs among existing nodes.
1	1	The agent node transmits successfully.
1	2	The agent node collides with existing nodes.

will omit the subscript 0 when it does not cause confusion. Here, $a_t = 1$ represents the transmission of a packet at slot t , while $a_t = 0$ indicates that the agent does not transmit at slot t and instead only listens to the channel.

2) *State*: After the agent takes action a_t , it receives a channel observation $o_t \in \{0, 1, 2\}$ from the feedback broadcasted by the AP. Here, $o_t = 0$ indicates no transmission on the channel, $o_t = 1$ indicates that only one node transmitted on the channel, and $o_t = 2$ indicates a collision caused by simultaneous transmission from multiple nodes. We denote the action-observation pair at time slot t as $h_t = (a_t, o_t)$, with five possible combinations for h_t , as summarized in Table I. Then, the state of the agent node can be defined using the past action-observation pairs in a history window to capture the temporal dynamics of the environment. Specifically, the state at time slot t is represented as $s_t = [h_{t-L}, h_{t-L+1}, \dots, h_{t-1}]$, where L is the length of the state history window.

3) *Reward*: The primary goal of the agent node is to maximize the total throughput of the entire network while ensuring fair coexistence with existing nodes. The reward related to throughput at time slot t is defined as follows:

$$r_t^p = \begin{cases} 1, & \text{if } o_t = 1, \\ 0, & \text{otherwise.} \end{cases} \quad (1)$$

This definition means that the agent node receives a reward when a packet is successfully transmitted at time slot t , whether the transmission is from the agent node or an existing node. However, no reward is given in the case of a collision or when the channel is idle.

To incorporate fairness considerations, we first define the short-term average throughput of the agent node and the existing nodes. Let $S_{t,0}$ denote the short-term average throughput of the agent node at time slot t , which is defined as the ratio of successful transmissions of the agent node within a window of Z time slots, i.e., $S_{t,0} = \frac{1}{Z} \sum_{t'=t-Z+1}^t r_{t'}^p a_{t'}$. As the agent node cannot distinguish the actual short-term average throughput of each existing node from the historical feedback provided by the AP, we treat the existing nodes as a collective entity and define the short-term average throughput of all existing node as $S_{t,N} = \frac{1}{Z} \sum_{t'=t-Z+1}^t r_{t'}^p (1 - a_{t'})$. Then, we design a reward function that accounts for both throughput and fairness as follows:

$$r_t = r_t^p \cdot (1 - \nu f_t), \quad (2)$$

where

$$f_t = \begin{cases} \frac{S_{t,0}}{S_{t,0} + S_{t,N}}, & \text{if } a_t = 1, \\ \frac{S_{t,N}}{S_{t,0} + S_{t,N}}, & \text{otherwise,} \end{cases} \quad (3)$$

and $\nu \in [0, 1]$ is the fairness factor.

By adjusting the value of ν , the reward function can balance throughput maximization and fairness considerations. A larger value of ν places greater emphasis on fairness, while a smaller value prioritizes throughput. When $\nu = 0$, the reward function focuses solely on the total network throughput. When $\nu = 1$, the reward can be rewritten as:

$$r_t = \begin{cases} \frac{S_{t,N}}{S_{t,0} + S_{t,N}}, & \text{if } (a_t, o_t) = (1, 1), \\ \frac{S_{t,0}}{S_{t,0} + S_{t,N}}, & \text{if } (a_t, o_t) = (0, 1), \\ 0, & \text{otherwise.} \end{cases} \quad (4)$$

When the agent node successfully transmits, the reward is proportional to the ratio of the existing nodes' throughput to the total network throughput. Conversely, if any existing node successfully transmits while the agent node remains silent, the reward is proportional to the ratio of the agent node's throughput to the total network throughput. This reward mechanism promotes fairness by guiding the agent node to seek transmission opportunities when its throughput is lower than that of the existing nodes, and encouraging it to yield access when its throughput exceeds that of existing nodes. In this way, the reward function helps minimize the throughput differences between the agent node and the existing nodes.

The goal of a conventional reinforcement learning problem is to find an optimal policy π^* that maximizes the expected sum of discounted rewards for a given task, as expressed by:

$$\pi^* = \arg \max_{\pi} \mathbb{E}_{\tau} \left[\sum_t \gamma^t r(s_t, a_t) \right], \quad (5)$$

where γ is the discount factor and τ is the trajectory induced by policy π . While the learned optimal policy performs well for a specific training task, its ability to generalize across different tasks is limited. In meta-RL, the problem is extended to a distribution of tasks $p(\mathcal{T})$. The training and test tasks are both drawn from this distribution, where each task \mathcal{T}^k corresponds to a different scenario, i.e., a distinct heterogeneous wireless network configuration. The key idea in meta-RL is to learn a policy that can generalize across a range of tasks, enabling the agent to quickly adapt to new tasks without needing to start from scratch. The goal of meta-RL is to find the optimal policy π^* that maximize the expected cumulative discounted reward over tasks drawn from the task distribution, which is expressed as:

$$\pi^* = \arg \max_{\pi} \mathbb{E}_{\mathcal{T}^k \sim p(\mathcal{T})} \left[\mathbb{E}_{\tau^k} \left[\sum_t \gamma^t r_t \right] \right], \quad (6)$$

where τ^k is the trajectory induced by policy π for task \mathcal{T}^k .

IV. META-RL-BASED GMA PROTOCOL

In this section, we first provide an overview of the proposed GMA protocol. Next, we describe the neural networks utilized within GMA. Finally, we outline the processes involved in both the meta-training and meta-testing phases.

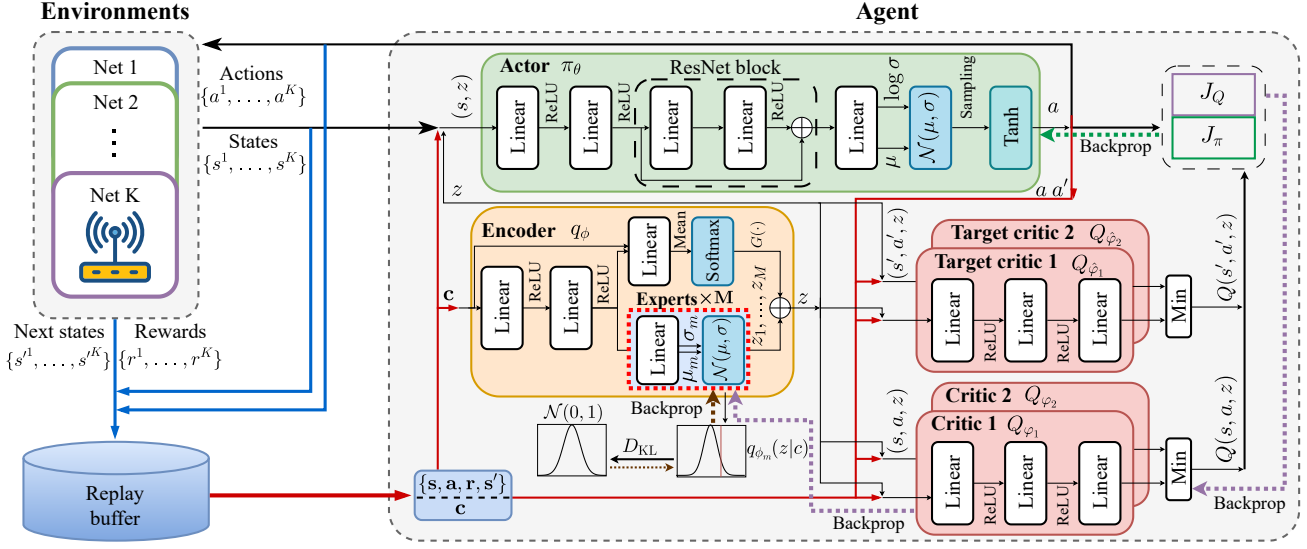


Fig. 2. The framework for GMA protocol.

A. Overview

We propose the GMA protocol, which leverages meta-RL techniques with MoE, to enhance the agent node’s ability to rapidly adapt and generalize across diverse heterogeneous network environments. Building on the PEARL framework from [21], [22], the GMA protocol includes an encoder [23] to generate task embeddings and uses SAC [24], [25] for learning a goal-conditioned policy. Unlike PEARL, we redesign the encoder architecture by incorporating an MoE layer [26], which allows for the generation of mixture latent representations from multiple experts. This enhancement enables the system to better differentiate between various tasks.

The encoder functions as an advanced feature extractor, distilling task-specific information from a set of recent transitions (state, action, reward, next state). Each transition is encoded using the MoE layer, producing a set of rich and diverse representations. These representations are then fused into a comprehensive task embedding, which is provided to SAC as the conditioning input. The MoE-enhanced encoder improves the system’s ability to distinguish between different tasks more effectively. SAC operates both as a policy function and an evaluation criterion. It utilizes an actor-critic architecture with separate policy and value function networks to learn the meta-policy using the task embeddings from the encoder. The actor generates task-specific actions based on both the current state and task representations, while the critic evaluates the performance of the conditioned policy. This structure enables the agent to adapt more efficiently to varying network conditions, thereby improving performance in meta-reinforcement learning scenarios. Further details are provided in the following subsections.

B. Neural Networks

As depicted in Fig. 2, the GMA protocol consists of several key components: an MoE-enhanced encoder network q_ϕ , an actor network π_θ , two critic networks Q_{φ_1} and Q_{φ_2} , and two

target critic networks Q_{φ_1} and Q_{φ_2} . Additionally, a replay buffer B is utilized to store the agent’s transitions (s, a, r, s') and facilitate the updating of network parameters.

Encoder network: The encoder network, parameterized by ϕ , is responsible for generating the task representation z based on the recent context $\mathbf{c} = \{c_1, c_2, \dots, c_U\}$, which comprises a set of transitions $c_u = (s, a, r, s')$ from the previous U time steps. The encoder combines a shared multilayer perceptron (MLP) backbone with an MoE layer, which includes a gating layer G and multiple experts $m \in \{1, 2, \dots, M\}$. The gating layer G consists of a linear layer followed by the Softmax activation to generate a set of weights:

$$G(\mathbf{c}) = \text{Softmax}\left(\frac{1}{U} \sum_{u=1}^U \text{Linear}(\text{MLP}(c_u), c_u)\right). \quad (7)$$

As shown in 3, each expert m is represented by a linear layer E_m , which independently encodes each individual transition c_u as a Gaussian factor $\Psi_{\phi,m}(z_m|c_u) = \mathcal{N}(\mu_m(c_u), \sigma_m(c_u))$. Here, $\mu_m(c_u)$ and $\sigma_m(c_u)$ denote the mean and variance of Gaussian factor, respectively. Given that the encoder is permutation-invariant [21], the Gaussian factors derived from each transition can be multiplied together to estimate the overall posterior of each expert m :

$$q_{\phi,m}(z|\mathbf{c}) \propto \prod_{u=1}^U \Psi_{\phi,m}(z|c_u). \quad (8)$$

The task representation z_m of each expert m is then sampled from $q_{\phi,m}(z|\mathbf{c})$. By weighting and combining the task representations from all experts using the weights $G_m(\mathbf{c})$ generated by gating layer G , the final mixture task representation is obtained as $z = \sum_{m=1}^M G_m(\mathbf{c})z_m$. The mixture task representation z serves as the conditioning input to SAC, facilitating effective learning and adaptation. For simplicity, we denote the overall process of task representation generation as $z \sim q_\phi(z|\mathbf{c})$.

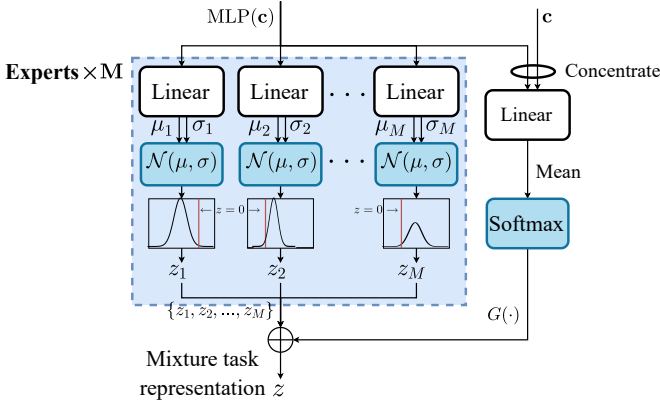


Fig. 3. MoE Probabilistic Embeddings.

Actor network: The actor network, parameterized by θ , generates actions a based on the current state s and the task representation z . It consists of an input layer, a ResNet block with a shortcut connection [27], and an output layer. The output of the actor network includes the mean μ and the log-variance $\log \sigma$ for the Tanh-normal distribution. From this distribution, we sample a continuous action \hat{a} that lies within the range of -1 to 1 . To obtain a discrete action, we apply a simple binary mapping to \hat{a} . Specifically, the action a is set to 1 if $\hat{a} \geq 0$, and 0 otherwise.

Critic networks: The two critic networks, parameterized by φ_1 and φ_2 , evaluate the value of an action taken in a given state and task representation by the actor. These critic networks are implemented as three-layer MLPs, with each outputting a parameterized soft Q-function denoted as:

$$Q_{\varphi_i}(s, a, z) = r + \gamma \mathbb{E}_{s' \sim p(\cdot|s, a)} [V_{\varphi_i}(s', z)], \quad (9)$$

where $p(\cdot|s, a)$ represents the state transition function. The soft state value function is defined as:

$$V_{\varphi_i}(s, z) = \mathbb{E}_{a \sim \pi} [Q_{\varphi_i}(s, a, z) - \alpha \log \pi(a|s, z)] \quad (10)$$

where α is the temperature parameter that controls the trade-off between policy entropy and reward. To mitigate overestimation of Q-values, the soft Q-function is estimated by taking the minimum of the outputs from the two critic networks, i.e., $\min(Q_{\varphi_1}(s, a, z), Q_{\varphi_2}(s, a, z))$ [28]. Additionally, two target critic networks, parameterized by $\hat{\varphi}_1$ and $\hat{\varphi}_2$, are employed to reduce the correlation between the target values and the current estimates of the critic networks, thereby enhancing the stability of the training process. Similar to the critic networks, the target critic networks are implemented as three-layer MLPs.

C. Procedure

The procedure consists of two phases: meta-training and meta-testing. In meta-training, the model learns a meta-policy by training on diverse tasks. During meta-testing, the model quickly adapts to new, unseen tasks using few-shot learning.

Meta-training: We consider a set of K training tasks $\{\mathcal{T}^k\}_{k=1, \dots, K}$, where each training task is drawn from the distribution $p(\mathcal{T})$. In each training episode, there are two phases:

Algorithm 1 Meta-Training of GMA Algorithm

Require: Training task set $\{\mathcal{T}^k\}_{k=1, \dots, K}$ from $p(\mathcal{T})$, learning rate $\lambda_\phi, \lambda_\pi, \lambda_\alpha, \lambda_Q$, soft update rate η , batch size N_E , collecting steps N_C

- 1: Initialize the parameters $\phi, \theta, \varphi_i, \hat{\varphi}_i$ ($i = 1, 2$) and α
- 2: Initialize replay buffer B^k for each task
- 3: **for** each episode **do**
- 4: **for all** \mathcal{T}^k **do**
- 5: Initialize environmental context $\mathbf{c}^k = \emptyset$
- 6: **for** $t = 1, 2, \dots, N_C$ **do**
- 7: Sample $z^k \sim q_\phi(z^k|\mathbf{c}^k)$
- 8: Gather transition (s_t, a_t, r_t, s_{t+1}) from $\pi_\theta(a|s, z^k)$ and store it into B^k
- 9: Sample $\mathbf{c}^k = \{(s_u, a_u, r_u, s'_u)\}_{u=1, \dots, N_E} \sim B^k$
- 10: **end for**
- 11: **end for**
- 12: **for** each gradient step **do**
- 13: Sample context and transition batches from $\{B^k\}_{k=1, \dots, K}$
- 14: Sample $z^k \sim q_\phi(z^k|\mathbf{c}^k)$ for all $k = 1, \dots, K$
- 15: Update networks:
 - 16: $\varphi_i \leftarrow \varphi_i - \lambda_Q \nabla_{\varphi_i} \sum_k J_Q(\varphi_i), i = 1, 2.$
 - 17: $\phi \leftarrow \phi - \lambda_\phi \nabla_\phi \sum_k J_{\text{en}}(\phi)$
 - 18: $\theta \leftarrow \theta - \lambda_\pi \nabla_\theta \sum_k J_\pi(\theta)$
 - 19: $\alpha \leftarrow \alpha - \lambda_{\text{temp}} \nabla_\alpha \sum_k J_{\text{temp}}(\alpha)$
 - 20: $\hat{\varphi}_i \leftarrow \eta \varphi_i + (1 - \eta) \hat{\varphi}_i, i = 1, 2.$
- 21: **end for**
- 22: **end for**

the data collection phase and the optimization phase. During the data collection phase, the agent collects training data from different training tasks. Specifically, for each training task, the agent leverages the encoder to derive the task representation z from the context \mathbf{c} , which is sampled uniformly from the most recently collected data in the current episode. Based on the task representation z and the state s , the agent generates an action a using the actor network. The resulting transitions are stored in individual replay buffers B^k for each training task k .

In the optimization phase, the loss functions for the encoder and SAC are computed, and the parameters of the encoder, actor, and critic networks are jointly updated using gradient descent. The critic networks Q_{φ_1} and Q_{φ_2} are updated by minimizing the soft Bellman error:

$$J_Q(\varphi_i) = \mathbb{E}_{\substack{(s, a, r, s') \sim B \\ z \sim q_\phi(z|\mathbf{c})}} \left[Q_{\varphi_i}(s, a, z) - \left(r + \gamma \left(\min_{i=1, 2} Q_{\hat{\varphi}_i}(s', a', z) - \alpha \log \pi_\theta(a'|s', z) \right) \right) \right]^2. \quad (11)$$

The target critic networks $Q_{\hat{\varphi}_1}$ and $Q_{\hat{\varphi}_2}$ are updated by:

$$\hat{\varphi}_i \leftarrow \eta \varphi_i + (1 - \eta) \hat{\varphi}_i, \quad i = 1, 2, \quad (12)$$

where η is the soft update rate.

The encoder's loss is defined based on the variational lower bound, which consists of two key components: the soft

Bellman error for the critic and the sum of the Kullback-Leibler (KL) divergence for each expert. Specifically, the loss function for the encoder is given by:

$$J_{\text{en}}(\phi) = \mathbb{E}_{\mathcal{T}} \left[\mathbb{E}_{z \sim q_{\phi}(z|c)} \left[\sum_{i=1}^2 J_Q(\varphi_i) + \beta \sum_{m=1}^M D_{\text{KL}}(q_{\phi,m}(z|c) \| p(z)) \right] \right], \quad (13)$$

where $p(z)$ is a unit Gaussian prior, $D_{\text{KL}}(\cdot|\cdot)$ is the KL divergence, and β is the weight the KL-divergence term. The KL divergence term for each expert is used to constrain the mutual information between the task representation z and the context c , ensuring that z contains only relevant information from the context and mitigating overfitting.

The loss utilized to update the actor network parameters is given by:

$$J_{\pi}(\theta) = \mathbb{E}_{s \sim B, a \sim \pi_{\theta}} \left[\alpha \log(\pi_{\theta}(a|s, z)) - \min_{i=1,2} Q_{\varphi_i}(s, a, z) \right]_{z \sim q_{\phi}(z|c)}. \quad (14)$$

The temperature parameter α is updated using the following loss function:

$$J_{\text{temp}}(\alpha) = \mathbb{E}_{s \sim B, a \sim \pi_{\theta}} \left[-\alpha \log(\pi_{\theta}(a|s, z)) - \alpha \bar{\mathcal{H}} \right]_{z \sim q_{\phi}(z|c)}, \quad (15)$$

where $\bar{\mathcal{H}}$ represents a target expected entropy, which is set to $-\dim(\mathcal{A})$ [25], and \mathcal{A} denotes the action space. The details of the meta-training process are summarized in Algorithm 1.

Meta-testing: In the meta-testing phase, the agent fine-tunes the actor and critic networks to adapt the policy to new tasks in a few-shot manner. The parameters of the encoder are fixed during this phase. When encountering a new task, the agent collects context data over a few time steps. The first transition is collected with task representation z sampled from the prior $q_{\phi}(z) = p(z)$. Subsequent transitions are collected with $z \sim q_{\phi}(z|c)$, where the context c is updated by selecting the latest U transitions. As more context is accumulated, the task representation z becomes increasingly accurate. The actor and critic networks are then updated using a procedure similar to that in the meta-training phase, enabling the agent to rapidly improve its performance on the new task. The details of the meta-testing process are summarized in Algorithm 2.

V. PERFORMANCE EVALUATION

In this section, we conduct extensive simulations using PyTorch to thoroughly evaluate the performance of the proposed GMA protocol. We first describe the simulation setup and then compare the performance of the proposed GMA protocol with two baseline protocols in different scenarios.

A. Simulation Setup

1) *Hyperparameters:* The state history length L is set to 20, the short-term average throughput window Z is set to 500, and the discount factor γ is set to 0.9. Unless otherwise specified, the fairness factor ν is set to a default value of 0. For the encoder network, the KL divergence weight β is set to 1,

Algorithm 2 Meta-Testing With Fine-Tuning

Require: Testing task $\mathcal{T}^{k'}$ from $p(\mathcal{T})$, fine-tuning time step set T_{ft} , meta-trained parameters $\theta, \phi, \varphi_i, \hat{\varphi}_i$ ($i = 1, 2$), learning rate $\lambda_{\pi}, \lambda_{\alpha}, \lambda_Q$, soft update factor η , batch size N_E , collecting steps N_c , context buffer size U

- 1: Initialize replay buffers $B^{k'}$, context $c^{k'} = \emptyset$, $\alpha, \theta^{k'} = \theta$, $\varphi_i^{k'} = \varphi_i, \hat{\varphi}_i^{k'} = \hat{\varphi}_i$ ($i = 1, 2$)
- 2: **for** $t = 1, 2, \dots, 3N_c$ **do**
- 3: Sample $z^{k'} \sim q_{\phi}(z^{k'}|c^{k'})$
- 4: Gather transition (s_t, a_t, r_t, s_{t+1}) from $\pi_{\theta^{k'}}(a|s, z^{k'})$ and store it into $B^{k'}$
- 5: Update context $c^{k'}$ with transition (s_t, a_t, r_t, s_{t+1})
- 6: **end for**
- 7: **for** remain episode length **do**
- 8: Sample $z^{k'} \sim q_{\phi}(z^{k'}|c^{k'})$
- 9: $a_t \sim \pi_{\theta^{k'}}(a_t|s_t, z^{k'})$
- 10: Execute a_t , receive $s_{t+1} \sim p(\cdot|s_t, a_t)$ and r_t
- 11: Update context $c^{k'}$ with transition (s_t, a_t, r_t, s_{t+1})
- 12: Store transition (s_t, a_t, r_t, s_{t+1}) into $B^{k'}$
- 13: **if** $t \in T_{\text{ft}}$ **then**
- 14: Sample transition batch from $B^{k'}$
- 15: Update networks:
- 16: $\varphi_i^{k'} \leftarrow \varphi_i^{k'} - \lambda_Q \nabla_{\varphi_i^{k'}} J_Q(\varphi_i^{k'})$, $i = 1, 2$.
- 17: $\theta^{k'} \leftarrow \theta^{k'} - \lambda_{\pi} \nabla_{\theta^{k'}} J_{\pi}(\theta^{k'})$
- 18: $\alpha \leftarrow \alpha - \lambda_{\text{temp}} \nabla_{\alpha} J_{\text{temp}}(\alpha)$
- 19: $\hat{\varphi}_i^{k'} \leftarrow \eta \varphi_i^{k'} + (1 - \eta) \hat{\varphi}_i^{k'}$, $i = 1, 2$.
- 20: **end if**
- 21: **end for**

the default number of experts M is set to 3, and the task representation dimension is set to 6. A replay buffer of size 1000 is used to store past experiences. Both transition and context batches are sampled with a batch size N_E of 64, and the context buffer size U is set to 150. Each hidden layer in the encoder, actor, and critic networks consists of 64 neurons with ReLU activation. The Adam optimizer with a learning rate of 0.003 is used to optimize all trainable parameters, and the soft update rate η is set to 0.005. During the meta-training phase, we collect data for a total of 200 steps for the GMA protocol ($N_c = 200$), while during the testing phase, we collect data for 50 steps ($N_c = 50$).

2) *Performance Metrics:* To evaluate the performance, we adopt $S_t = S_{t,0} + S_{t,N}$ as the throughput metric. We also employ Jain's index [29] as a fairness metric in Section V-G. Jain's index is defined as $\frac{S_{t,0}^2 + S_{t,N}^2}{2(S_{t,0}^2 + S_{t,N}^2)}$, which quantifies the fairness of throughput distribution between the agent node and existing nodes. For consistency, all simulation results are averaged over 10 independent experiments per scenario, and Jain's index is computed based on these averaged short-term throughput values.

3) *Baseline Protocols:* We compare the performance of the proposed GMA protocol with the following baseline protocols:

- DLMA: The agent node accesses the channel using the DLMA protocol [4].
- DLMA-SAC: This baseline is a variant of DLMA, where

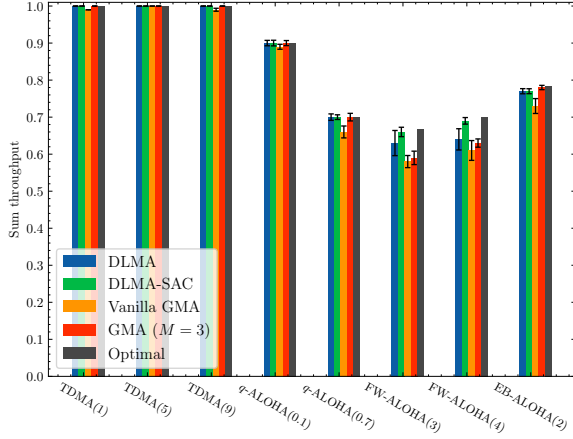


Fig. 4. Comparison of the performance of different protocols in various training environments. Each experiment was conducted over 20,000 time slots, with error bars representing the standard deviations from 10 simulations per case.

the original DQN component is replaced with the SAC.

- Vanilla GMA: A specific variant of GMA, where the number of experts M is set to 1 [1].
- Optimal policy: This baseline assumes that the agent node has complete knowledge of the MAC mechanisms employed by existing nodes in the network, providing the optimal network throughput as the benchmark [4].

To ensure a fair comparison, all algorithms are designed with neural networks of similar parameter counts for decision making. This allows us to focus on the differences in their learning algorithms and evaluate their relative performance in a consistent manner.

4) *Notations*: To distinguish between different scenarios in heterogeneous wireless networks, we introduce a notation system based on the protocols and settings employed. The following notations are defined:

- q -ALOHA(q): A scenario with a single existing node using the q -ALOHA protocol for access, where the transmission probability is denoted by q .
- FW-ALOHA(W): A scenario with a single existing node using the FW-ALOHA protocol, where the window size is fixed at W .
- EB-ALOHA(W): A scenario where a single existing node employs the EB-ALOHA protocol, with an initial window size W and a maximum backoff stage $b = 2$.
- TDMA(X): A scenario where a single existing node transmits in the specified slot X within a frame consisting of 10 slots.

B. Meta-training Performance

A set of training tasks is employed for meta-training. Specifically, eight distinct environments are considered, including three TDMA environments with time slots X of 1, 5, and 9, two q -ALOHA environments with transmission probabilities q of 0.1 and 0.7, two FW-ALOHA environments with window sizes W of 3 and 4, and one EB-ALOHA environment with an initial window size W of 2.

The performance of different MAC protocols in various training environments is shown in Fig. 4. The DLMA and DLMA-SAC nodes are trained from scratch in each environment during the training phase, while both the vanilla GMA and GMA node are trained on all environments in the training task set. For simplicity, we refer to both versions of GMA (vanilla and with multiple experts) as "GMA" in subsequent references. The simulation results demonstrate that the GMA protocol performs well across multiple environments, with only slight performance degradation compared to the DLMA and DLMA-SAC protocols, which are optimized for specific environments. In addition, GMA with additional experts provides more stability and higher performance than the vanilla GMA due to its improved representation.

C. Meta-testing Performance

In the testing phase, we evaluate the generalization capabilities of the proposed GMA protocol on new tasks that were not encountered during the training phase. We consider a total of six environments: four with a single coexisting nodes and two with multiple coexisting nodes. The single-node environments are TDMA(5), q -ALOHA(0.8), FW-ALOHA(2), and EB-ALOHA(3). These environments represent different MAC protocols and settings, including TDMA with a time slot of 5, q -ALOHA with a transmission probability of 0.8, FW-ALOHA with a window size of 2, and EB-ALOHA with a window size of 3. The multi-node environments include one with TDMA(2) and q -ALOHA(0.1), and another with TDMA(3) and q -ALOHA(0.6). These environments involve combinations of TDMA and q -ALOHA protocols with different time slots and transmission probabilities.

In each testing environment, agents collect transitions during the first 150 time steps to fill the replay buffer. During this period, the GMA agent also accumulates context information. After 150 time steps, all agents begin the fine-tuning or training phase. The GMA agent is updated every 50 time steps, while the DLMA and DLMA-SAC agents are updated every 5 time steps. After the 300th time step, the GMA agent completes its fine-tuning, while the DLMA and DLMA-SAC agents continue updating. Note that all hyperparameters used during the testing phase are consistent with those used in the training phase.

As illustrated in Fig. 5, the GMA agent exhibits rapid convergence towards a near-optimal access strategy after just three updates in all testing environments. In contrast, the DLMA and DLMA-SAC agents perform poorly at first and fail to converge within the given time duration, despite undergoing ten times as many updates. This highlights the GMA protocol's significant advantage in adapting to new environments compared to previous DRL protocols trained from scratch. Moreover, the GMA agent achieves higher sum throughput compared to the other two baseline protocols. This is because the GMA agent leverages the task representation extracted by the encoder and utilizes the knowledge learned from previous environments to quickly identify the optimal access strategy. Although the GMA agent was trained on simpler tasks with single-node environments, it shows remarkable initial performance and

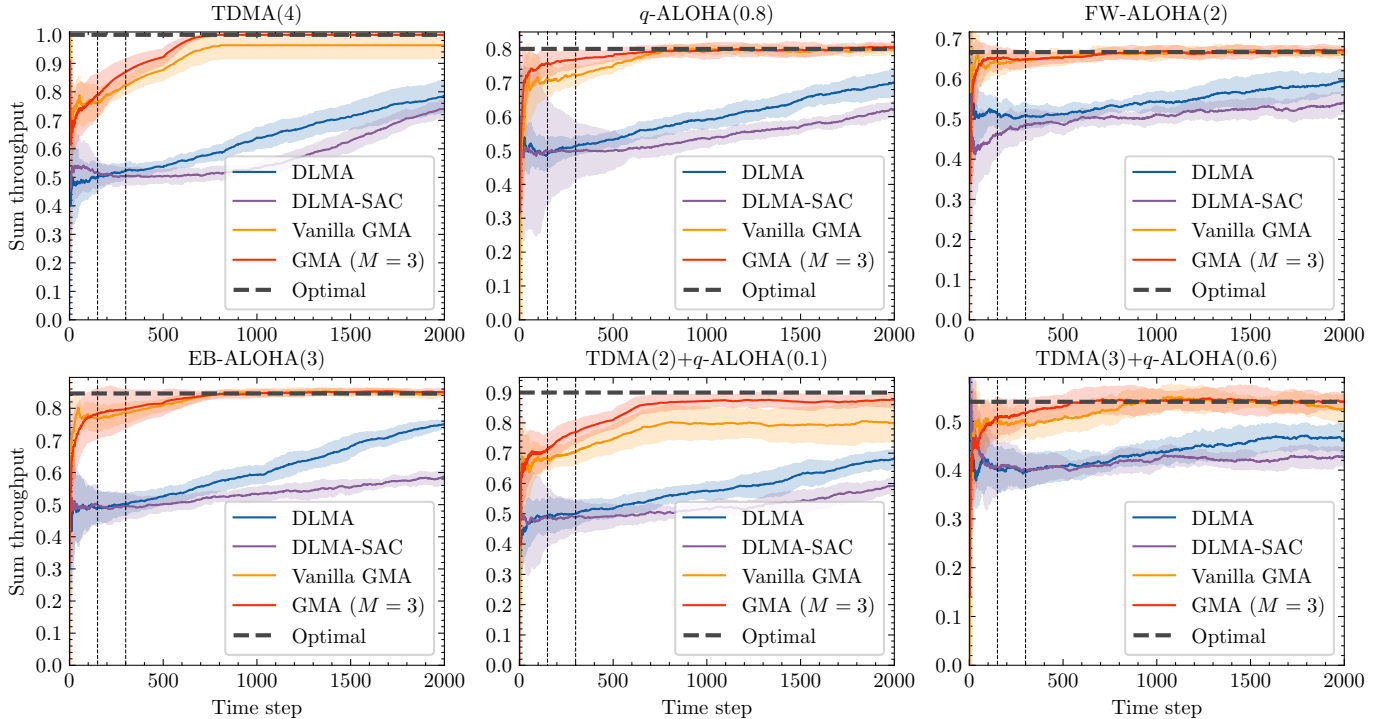


Fig. 5. Comparison of the performance of different protocols in various testing environments. The first vertical dashed line at the 150th time step marks the beginning of agents’ fine-tuning or training, while the second vertical dashed line indicates the completion of the fine-tuning for the GMA agent. The DLMA and DLMA-SAC agents continue updating beyond this point. The shaded area around the curves represents the standard deviations from 10 experiments.

few-shot capabilities when handling multi-node environments. Additionally, due to the incorporation of the MoE architecture, the GMA achieves higher initial performance and converges faster compared to the vanilla GMA. It indicates that the MoE architecture enhances representation learning, allowing the agent to better leverage prior knowledge and adapt more efficiently to new environments.

Next, we evaluate the rapid adaptability of the proposed GMA protocol in a dynamic environment, where the number of existing nodes and their protocols change every 2000 time slots. Both DLMA and DLMA-SAC agents are trained in the TDMA(7) environment, while the GMA agent is initialized with the model obtained from meta-training. All agents are updated every 50 time steps. After each environmental change, GMA updates only 16 times, whereas DLMA and DLMA-SAC continue updating. The initial scenario we investigate involves the agent coexisting with one TDMA(4) node. At the 2000th time slot, a q -ALOHA node with a transmission probability q of 0.1 joins, the agent must coexist with one q -ALOHA node and one TDMA node with a time slot 2. At the 4000th time slot, the assigned slot X for TDMA changes from 2 to 3, and the transmission probability of q -ALOHA increases from 0.1 to 0.2. At the 6000th time slot, the TDMA and q -ALOHA nodes leave, and one FW-ALOHA node with a window size of 2 joins. As depicted in Fig. 6, our protocol quickly adapts to environmental changes and re-learns a near optimal access strategy. While the DLMA and DLMA-SAC fail to track the environmental changes and need more updates to converge, it demonstrates that our protocol achieves significantly faster convergence in a dynamic environment and

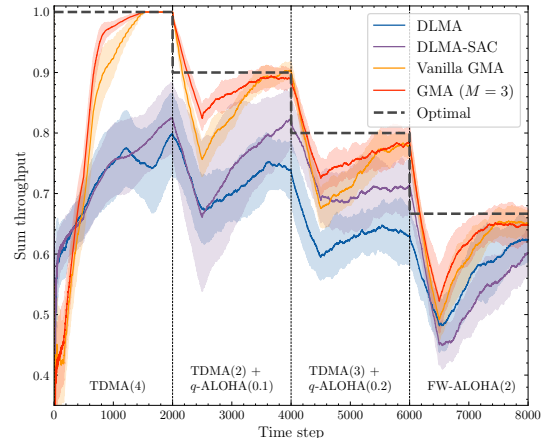


Fig. 6. Sum throughput in a dynamic environment.

can rapidly adapt to changes. Furthermore, compared to the vanilla GMA, the GMA with three experts adapts more rapidly, showing the benefits of expert diversity.

D. The Impact of the Size of the Meta-training Set

In this subsection, we analyze the generalization capabilities of the proposed GMA protocol by varying the size of the meta-training sets. Specifically, as illustrated in Fig. 7, we investigate the impact of increasing the number of q -ALOHA tasks and TDMA tasks within these sets. On the left side of the figures (before the vertical dashed line), we present a series of q -ALOHA environments with transmission probabilities

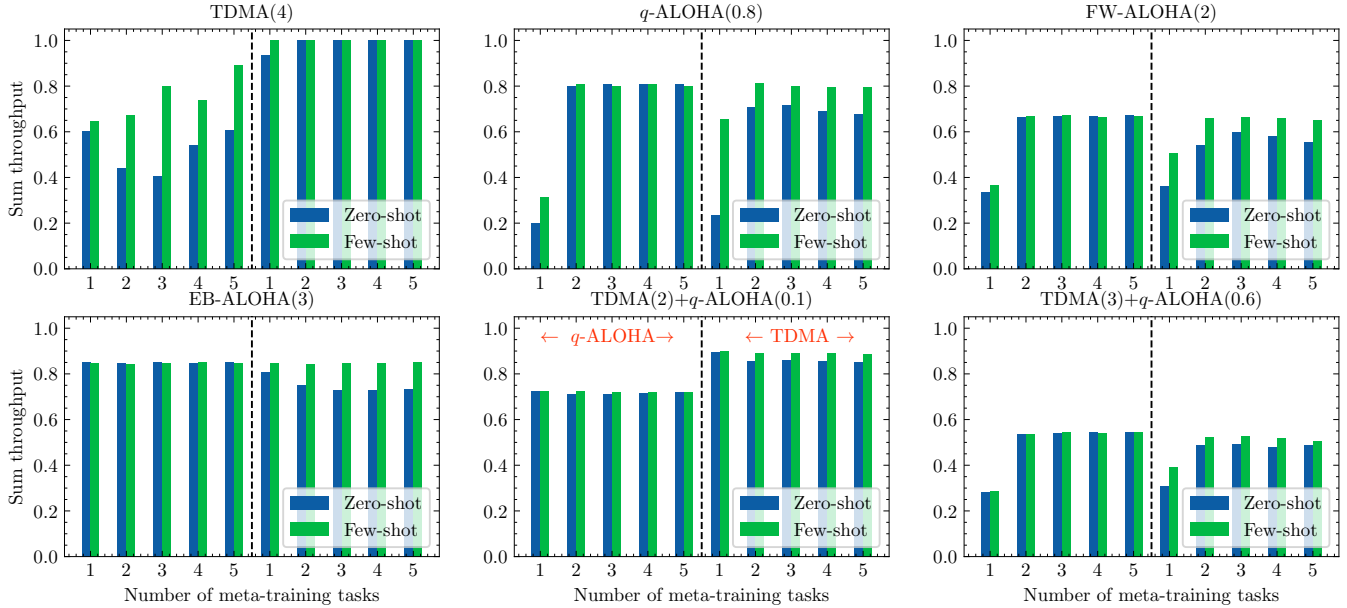


Fig. 7. A performance comparison with an increasing number of meta-training tasks. The left side of the vertical dashed line represents a set of q -ALOHA tasks, while the right side represents a set of TDMA tasks. Each meta-training set consists of distinct tasks, and the x -axis represents the size of the set.

q of 0.1, 0.7, 0.5, 0.3, and 0.9. The x -axis indicates the cumulative inclusion of environments in the meta-training set (e.g., the value of 2 on the x -axis corresponds to the first two environments with q values of 0.1 and 0.7). Correspondingly, on the right side of the vertical dashed line, we investigate multiple TDMA environments with time slots X of 1, 9, 5, 3, and 7, following the same x -axis representation. As in Section V-C, we assess the influence of the training set size by evaluating adaptation performance across six distinct environments during the meta-testing phase.

Fig. 7 illustrates the zero-shot and few-shot performance as the number of training tasks increases. In general, an increase in the number of tasks during meta-training leads to an overall improvement in zero-shot performance. However, there is a threshold beyond which further gains are limited due to model size constraints. As a result, the performance might fall short of the level achieved by the optimal strategy. Comparing the adaptation performance in the six distinct environments between the TDMA and q -ALOHA meta-training sets, we observe that the composition of the meta-training set directly influences zero-shot performance. The meta-trained model shows higher generalization performance when the adaptation tasks closely resemble those in the training set. Furthermore, Fig. 7 shows that for environments with TDMA nodes, models meta-trained on pure TDMA sets outperform those trained on q -ALOHA sets. Conversely, for environments with only ALOHA nodes, models meta-trained on pure q -ALOHA sets perform better than those trained on TDMA sets. For environments with multiple existing nodes, the environment features tend to be dominated by the transmission characteristics of a certain dominant node. Therefore, the similarity between the meta training task set and this dominant node determines the testing performance in such environments. Additionally, with three-step fine-tuning, models meta-trained

on pure TDMA sets achieve near-optimal performance across various environments, while models meta-trained on pure q -ALOHA sets may fail to converge in some environments. The GMA protocol demonstrates the ability to rapidly generalize to new tasks, even with a smaller number of tasks in the training set, reducing sampling and model update costs.

E. The Impact of the Diversity of the Meta-training Set

In this subsection, we evaluate the generalization capabilities of the proposed GMA protocol in terms of performance, considering the diversity of tasks in the meta-training sets. The meta-training sets consist of a fixed number of 8 distinct tasks. The sets in Fig. 8 are defined as follows:

- Set 1: Eight TDMA environments with time slots X of 1, 2, 3, 5, 6, 7, 8, and 9 are considered.
- Set 2: Six TDMA environments with time slots X of 1, 3, 5, 6, 7, and 9, and two q -ALOHA environments with transmission probabilities q of 0.1 and 0.7 are considered.
- Set 3: Five TDMA environments with time slots X of 1, 5, 6, 7, and 9, two q -ALOHA environments with transmission probabilities q of 0.1 and 0.7, and one EB-ALOHA environment with a window size W of 2 are considered.
- Set 4: Three TDMA environments with time slots X of 1, 5, and 9, two q -ALOHA environments with transmission probabilities q of 0.1 and 0.7, two FW-ALOHA environments with window sizes W of 3 and 4, and one EB-ALOHA environment with a window size W of 2 are considered.

As the set index increases, the diversity of the meta-training sets also increases. By examining the adaptation performance of the GMA protocol across these sets, we can gain insights into how the diversity and complexity of tasks impact the

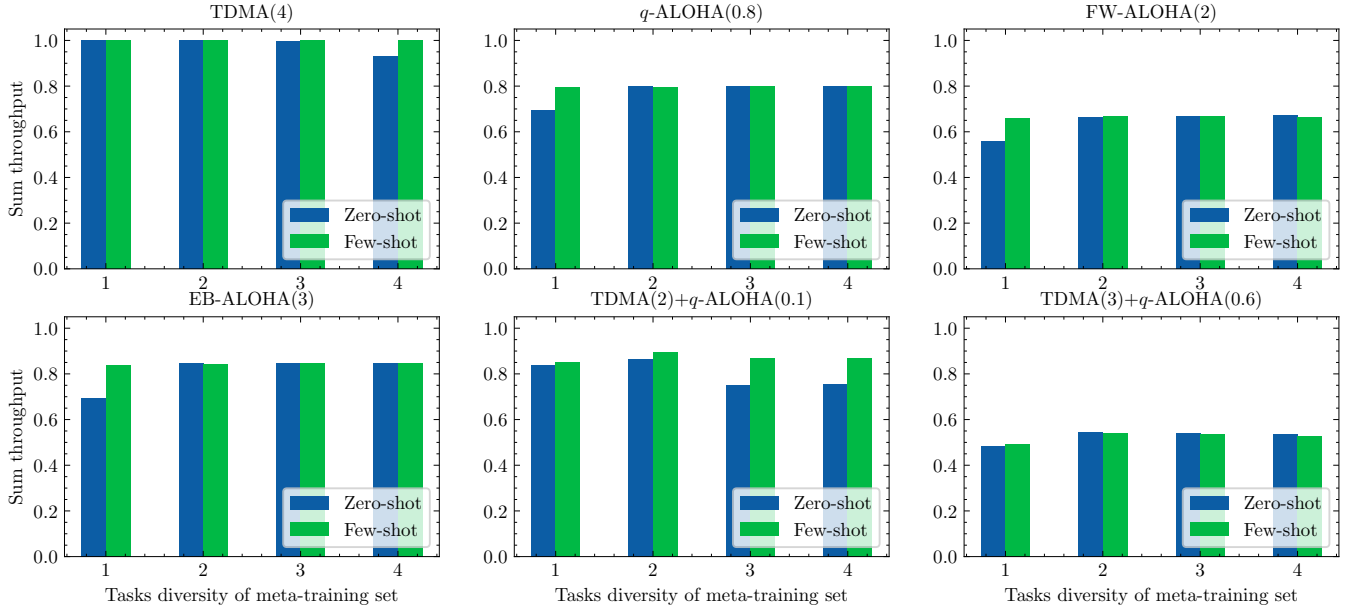


Fig. 8. Meta-training with gradual increases in the diversity of training tasks set, the x -axis represents the set index.

generalization abilities of the model. As in Section V-C, we evaluate the impact of task diversity by analyzing the adaptation performance across six distinct environments during the meta-testing phase.

As shown in Fig. 8, increasing the diversity of the meta-training set during the meta-training stage leads to improved initial performance in a larger number of environments during the meta-testing stage. This can be attributed to the fact that a more diverse meta-training set allows the encoder to learn to differentiate between environments with different types of features and develop a more comprehensive understanding of how to interact with diverse features. Consequently, higher diversity facilitates better matching of features in new environments during the meta-testing stage, enabling the agent to leverage similar feature experiences for improved adaptation. However, it is important to note that increased diversity does not always benefit specific environments. For instance, in the case of TDMA(4), the zero-shot performance actually decreases as the diversity increases. This is because although the overall diversity increases, the diversity specifically within the "TDMA" category decreases. This aligns with the expected results discussed earlier. Therefore, the measure of diversity in the meta-training set should be carefully considered based on the distribution of different environments that need to be adapted to. Additionally, the selection of the meta-training set directly impacts the cost of deployment. Increasing diversity typically comes at the expense of increased sampling and model update costs. Therefore, it's crucial to strike a balance between diversity and practical considerations such as resource constraints and deployment efficiency.

F. The Impact of the Number of Experts

In this subsection, we investigate the effect of the number of experts, M . Both the training set and testing set are the same as those described in Sections V-B and V-C. As shown

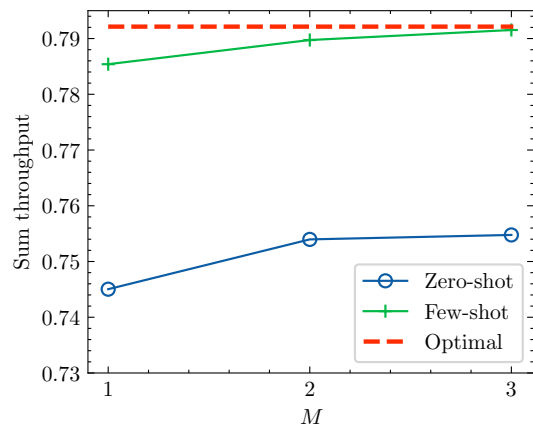


Fig. 9. GMA with different number of experts M .

in Fig. 9, both zero-shot and few-shot performance improve as the number of experts M increases, reaching near-optimal performance when $M = 3$.

To better understand this effect, we analyze the behavior of the agent from the perspective of dominant nodes. In environments such as q -ALOHA(0.8), FW-ALOHA(2), and "TDMA(3)+ q -ALOHA(0.6)", the existing nodes dominate the overall throughput [4], which results in the agent node opting not to transmit, as it aims to avoid contention. Conversely, in "TDMA(2)+ q -ALOHA(0.1)" and EB-ALOHA(3), the agent node is responsible for the majority of the throughput and, as a result, transmits more frequently to maximize performance [4]. As illustrated in Fig. 10, when $M = 1$, similar behavior patterns of the agent in different environments are only loosely grouped, indicating a lack of precision in the learned representation. However, as M increases, the representation becomes more distinct and well-clustered, suggesting that the use of additional experts allows for better differentiation between

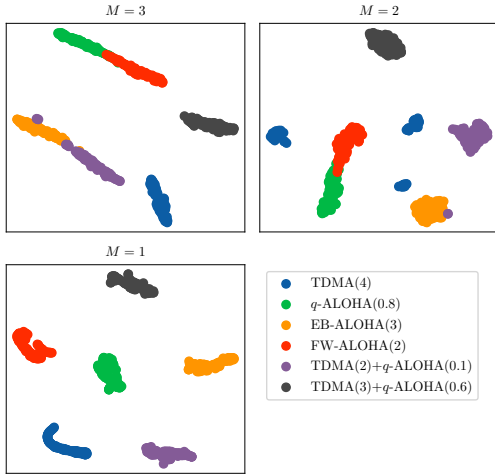


Fig. 10. The t-SNE visualization of latent representations extracted from trajectories collected in the meta-testing environments with different number of experts M .

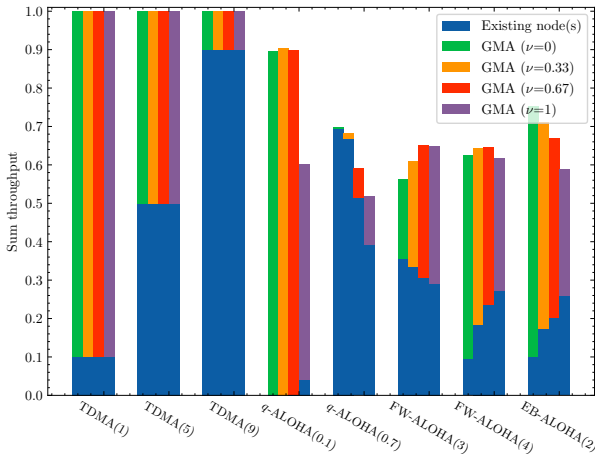


Fig. 11. Meta-training with different fairness factor ν .

various behaviors. This improvement in clustering reflects enhanced representation learning, which directly contributes to the agent’s ability to adapt effectively across diverse network environments.

G. Fair Coexistence Objective with Existing Nodes

In previous subsections, our primary focus was on maximizing total throughput. However, we recognized a potential issue with this criterion, as certain nodes may face difficulties accessing the network in specific environments. To address this concern, we evaluate the reward function with fairness consideration. In this subsection, we maintained the same meta-training and meta-testing sets, as well as the hyperparameters, except for the fairness factor ν as described in Section V-B. The results presented in Fig. 11 and Fig. 12 demonstrate the relationship between the fairness factor ν and the throughput. As ν increases, the throughput of the “disadvantaged” nodes exhibits a noticeable improvement, indicating that our proposed approach effectively enhances fairness among the agent node and existing nodes.

As shown in Fig. 11, when considering static scheduling environments such as TDMA, increasing the value of ν does not have a significant impact on the actual access strategies. This observation can be attributed to the fact that, in static environments, collisions are the primary factor contributing to the Jain’s index. However, under our specified reward scheme, collisions do not result in higher cumulative rewards. This aligns with the practical consideration that introducing unnecessary collisions to ensure fairness is not meaningful. Therefore, the reward design we propose is consistent with the requirements of static scheduling environments. However, in environments with certain randomness and opportunistic access, we observe that as ν increases, the throughput of nodes that were previously unable to access in the scenario of maximizing throughput gradually improves, indicating that they are given the opportunity to access. Moreover, from the graph, we can see that in some environments, increasing fairness among nodes can lead to an increase in overall throughput. For certain environments, an appropriate fairness metric allows the agent to overcome local optima issues and approach the optimal strategy more effectively. Integrating appropriate fairness factors ν during training is more conducive to achieving more reasonable access in various environments.

Similarly, as shown in Fig. 12, in certain environments, a reasonable fairness factor allows the agent to trade off a slight decrease in throughput for a significant increase in fairness, as represented by the Jain’s index.

VI. CONCLUSION

In this study, we proposed a generalizable MAC protocol utilizing meta-RL to tackle the challenge of generalizing multiple access in various heterogeneous wireless networks. Specifically, we introduced a novel meta-RL approach that incorporates a MoE architecture into the representation learning of the encoder. By combining the MoE-enhanced encoder and SAC techniques, the proposed GMA protocol effectively learns task information by capturing latent context from recent experiences, enabling rapid adaptation to new environments. This protocol hence holds great promise for enhancing spectrum efficiency and achieving efficient coexistence in heterogeneous wireless networks. Through extensive simulations, we demonstrated that the GMA protocol achieves universal access in training environments, with only a slight performance loss compared to baseline methods specifically trained for each environment. Furthermore, the GMA protocol exhibits faster convergence and higher performance in new environments compared to baseline methods. These results highlight the GMA protocol’s capability to dynamically adapt to different network scenarios and optimize spectrum utilization.

REFERENCES

- [1] Z. Liu, X. Wang, Y. Zhang, and X. Chen, “Meta Reinforcement Learning for Generalized Multiple Access in Heterogeneous Wireless Networks,” in *Proc. IEEE Wiopt Workshop Mach. Learn. Wireless Commun. (WMLC)*, Aug. 2023, pp. 570–577.
- [2] “DARPA SC2 Website,” <https://spectrumcollaborationchallenge.com/>.
- [3] P. Tilghman, “Will rule the airwaves: A DARPA grand challenge seeks autonomous radios to manage the wireless spectrum,” *IEEE Spectrum*, vol. 56, no. 6, pp. 28–33, Jun. 2019.

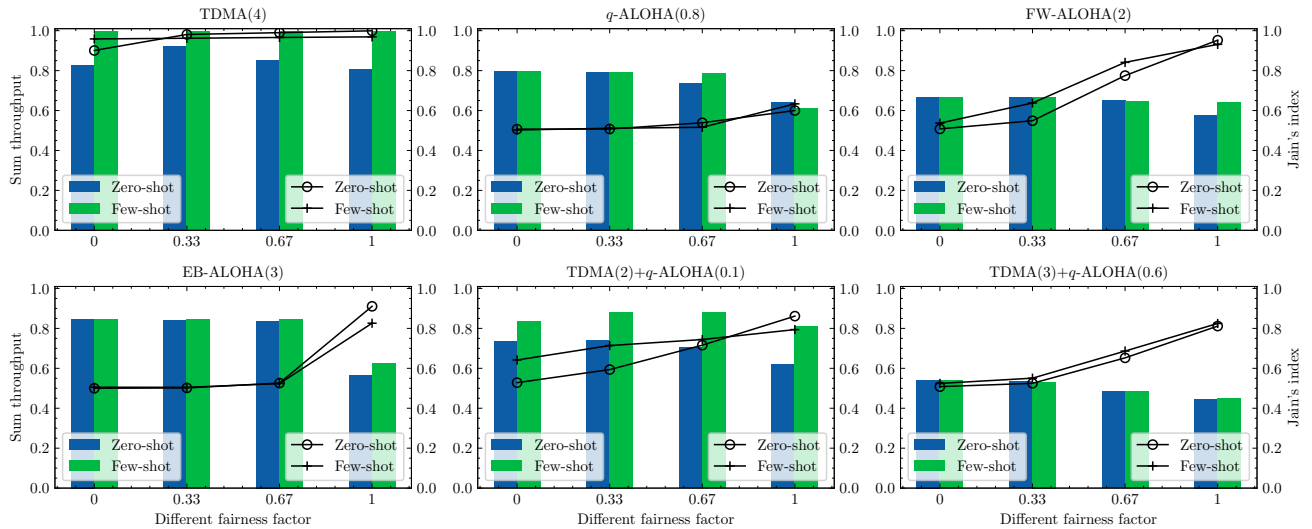


Fig. 12. Meta-testing with different fairness factor ν . In these figures, the bars represent the sum throughput, while the lines indicate the Jain's index.

- [4] Y. Yu, T. Wang, and S. C. Liew, "Deep-Reinforcement Learning Multiple Access for Heterogeneous Wireless Networks," *IEEE J. Sel. Areas Commun.*, vol. 37, no. 6, pp. 1277–1290, Jun. 2019.
- [5] X. Ye, Y. Yu, and L. Fu, "Multi-Channel Opportunistic Access for Heterogeneous Networks Based on Deep Reinforcement Learning," *IEEE Trans. Wireless Commun.*, vol. 21, no. 2, pp. 794–807, Feb. 2022.
- [6] Y. Yu, S. C. Liew, and T. Wang, "Non-Uniform Time-Step Deep Q-Network for Carrier-Sense Multiple Access in Heterogeneous Wireless Networks," *IEEE Trans. Mobile Comput.*, vol. 20, no. 9, pp. 2848–2861, Sep. 2021.
- [7] H. Xu, X. Sun, H. H. Yang, Z. Guo, P. Liu, and T. Q. S. Quek, "Fair Coexistence in Unlicensed Band for Next Generation Multiple Access: The Art of Learning," in *Proc. IEEE Int. Conf. on Commun. (ICC)*, May 2022, pp. 2132–2137.
- [8] X. Ye, Y. Yu, and L. Fu, "Deep Reinforcement Learning Based MAC Protocol for Underwater Acoustic Networks," *IEEE Trans. Mobile Comput.*, vol. 21, no. 5, pp. 1625–1638, May 2020.
- [9] X. Geng and Y. R. Zheng, "Exploiting Propagation Delay in Underwater Acoustic Communication Networks via Deep Reinforcement Learning," *IEEE Trans. Neural Netw. Learn. Syst.*, vol. 34, no. 12, pp. 10626–10637, 2023.
- [10] L. Deng, D. Wu, Z. Liu, Y. Zhang, and Y. S. Han, "Reinforcement Learning for Improved Random Access in Delay-Constrained Heterogeneous Wireless Networks," *arXiv:2205.02057*, May 2022. [Online]. Available: <http://arxiv.org/abs/2302.07837>
- [11] Y. Yu, S. C. Liew, and T. Wang, "Multi-Agent Deep Reinforcement Learning Multiple Access for Heterogeneous Wireless Networks With Imperfect Channels," *IEEE Trans. Mobile Comput.*, vol. 21, no. 10, pp. 3718–3730, Oct. 2022.
- [12] L. Lu, X. Gong, B. Ai, N. Wang, and W. Chen, "Deep Reinforcement Learning for Multiple Access in Dynamic IoT Networks Using Bi-GRU," in *Proc. IEEE Int. Conf. on Commun. (ICC)*, May 2022, pp. 3196–3201.
- [13] M. Han, Z. Chen, and X. Sun, "Multiple access via curriculum multi-task happe based on dynamic heterogeneous wireless network," *IEEE Internet Things J.*, vol. 11, no. 21, pp. 35073–35085, 2024.
- [14] V. Mnih, K. Kavukcuoglu, D. Silver, A. A. Rusu, J. Veness, M. G. Bellemare, A. Graves, M. Riedmiller, A. K. Fidjeland, G. Ostrovski, S. Petersen, C. Beattie, A. Sadik, I. Antonoglou, H. King, D. Kumaran, D. Wierstra, S. Legg, and D. Hassabis, "Human-level control through deep reinforcement learning," *Nature*, vol. 518, no. 7540, pp. 529–533, Feb. 2015.
- [15] Z. Guo, Z. Chen, P. Liu, J. Luo, X. Yang, and X. Sun, "Multi-Agent Reinforcement Learning-Based Distributed Channel Access for Next Generation Wireless Networks," *IEEE J. Sel. Areas Commun.*, vol. 40, no. 5, pp. 1587–1599, May 2022.
- [16] F. Frommel, G. Capdehourat, and F. Larroca, "Reinforcement Learning Based Coexistence in Mixed 802.11ax and Legacy WLANs," in *Proc. IEEE Wireless Commun. Netw. Conf. (WCNC)*, Mar. 2023, pp. 1–6.
- [17] E. Pei, Y. Huang, L. Zhang, Y. Li, and J. Zhang, "Intelligent Access to Unlicensed Spectrum: A Mean Field based Deep Reinforcement Learning Approach," *IEEE Trans. Wireless Commun.*, vol. 22, no. 4, pp. 2325–2337, Apr. 2023.
- [18] J. Xiao, H. Xu, X. Sun, F. Luo, and W. Zhan, "Maximum Throughput in the Unlicensed Band under 3GPP Fairness," in *Proc. IEEE/CIC Int. Conf. Commun. China (ICCC)*. IEEE, Aug. 2022, pp. 798–803.
- [19] J. Tan, L. Zhang, Y.-C. Liang, and D. Niyato, "Deep Reinforcement Learning for the Coexistence of LAA-LTE and WiFi Systems," in *Proc. IEEE Int. Conf. on Commun. (ICC)*, May 2019, pp. 1–6.
- [20] M. A. Jadoon, A. Pastore, M. Navarro, and F. Perez-Cruz, "Deep Reinforcement Learning for Random Access in Machine-Type Communication," in *Proc. IEEE Wireless Commun. Netw. Conf. (WCNC)*, Apr. 2022, pp. 2553–2558.
- [21] K. Rakelly, A. Zhou, C. Finn, S. Levine, and D. Quillen, "Efficient Off-Policy Meta-Reinforcement Learning via Probabilistic Context Variables," in *Proc. Int. Conf. Mach. Learn. (ICML)*. PMLR, May 2019, pp. 5331–5340.
- [22] F. Retyk, "On Meta-Reinforcement Learning in task distributions with varying dynamics," Master's thesis, Universitat Politècnica de Catalunya, Apr. 2021.
- [23] D. P. Kingma and M. Welling, "Auto-Encoding Variational Bayes," *arXiv:1312.6114*, May 2014. [Online]. Available: <http://arxiv.org/abs/1312.6114>
- [24] T. Haarnoja, A. Zhou, P. Abbeel, and S. Levine, "Soft Actor-Critic: Off-Policy Maximum Entropy Deep Reinforcement Learning with a Stochastic Actor," in *Proc. Int. Conf. Mach. Learn. (ICML)*. PMLR, Jul. 2018, pp. 1861–1870.
- [25] T. Haarnoja, A. Zhou, K. Hartikainen, G. Tucker, S. Ha, J. Tan, V. Kumar, H. Zhu, A. Gupta, P. Abbeel, and S. Levine, "Soft Actor-Critic Algorithms and Applications," *arXiv:1812.05905*, Jan. 2019. [Online]. Available: <http://arxiv.org/abs/1812.05905>
- [26] S. E. Yüksel, J. N. Wilson, and P. D. Gader, "Twenty years of mixture of experts," *IEEE Trans. Neural Networks Learn. Syst. (TNNLS)*, vol. 23, no. 8, pp. 1177–1193, 2012.
- [27] K. He, X. Zhang, S. Ren, and J. Sun, "Deep residual learning for image recognition," in *Proc. IEEE Conf. Comput. Vis. Pattern Recog. (CVPR)*, 2016, pp. 770–778.
- [28] H. Hasselt, "Double Q-learning," in *Proc. Adv. Neural Inf. Process. Syst. (NeurIPS)*, vol. 23, 2010.
- [29] R. K. Jain, D.-M. W. Chiu, W. R. Hawe *et al.*, "A quantitative measure of fairness and discrimination," *Eastern Res. Lab., Digit. Equip. Corp., Hudson, MA, USA, Tech. Rep.*, vol. 21, 1984.